Research article

Conformational preferences of cationic β-peptide in water studied by CCSD(T), MP2, and DFT methods

Young Kee Kang [a,*], Hae Sook Park [b]

[a] Department of Chemistry, Chungbuk National University, Cheongju, Chungbuk 28644, Republic of Korea
[b] Department of Nursing, Cheju Halla University, Cheju 63092, Republic of Korea

ABSTRACT

The conformational preferences of the cationic nylon-3 βNM [(3R,4)-diaminobutanoic acid, dAba] dipeptide in water were explored as the first step to understand the mode of action of polymers of βNM against phylogenetically diverse and intrinsically drug-resistant pathogenic fungi. The CCSD(T), MP2, M06-2X, ωB97X-D, B2PLYP-D3BJ, and DSD-PBEP86-D3BJ levels of theory with various basis sets were assessed for relative energies of the 45 local minima of the cationic Ac-dAba-NHMe located at the SMD M06-2X/6-31+G(d) level of theory in water against the benchmark CCSD(T)/CBS-limit energies in water. The best performance was obtained at the double-hybrid DSD-PBEP86-D3BJ/def2-QZVP level of theory with RMSD = 0.12 kcal/mol in water. The M06-2X/def2-QZVP level of theory predicted reasonably the conformational preference with RMSD = 0.38 kcal/mol in water and may be an alternative level of theory with marginal deviations for the calculation of conformational energies of relatively longer cationic peptides in water. In particular, the H_{14}–helical structures appeared to be the most feasible conformations for the cationic Ac-dAba-NHMe populated at 48–64% by relative free energies in water. The hexamer built from the H_{14}–structure of the cationic Ac-dAba-NHMe adopted a left-handed 3_{14}-helix, which has a slightly narrower radius and a longer rise than the regular 3_{14}-helix of β-peptides. Hence, the 3_{14}-helices of oligomers or polymers of the cationic dAba residues are expected to be the active conformation to exhibit the ability to bridge between charged lipid head groups that might cause a local depression or invagination of the membrane of fungi.

1. Introduction

For two decades, the density functional theory (DFT) has been an efficient computational tool in conformational study of amino acids and peptides [1, 2, 3, 4, 5, 6]. Compared to correlated wave function theories, DFT has achieved a better performance. However, further investigation on higher levels of theory with electron correlations and large basis sets are necessary in order to describe non-covalent interactions in peptides.

Multiple attempts have been made using the complete basis set (CBS) extrapolation and CCSD(T) corrections to reproduce accurately (~1 kcal/mol) experimental thermochemical data, barrier heights of chemical reactions, and non-covalent interaction energies [3, 7]. However, the computational cost was a limiting factor when applying CCSD(T)/CBS methods to conformational study of amino acids [8, 9, 10] and small peptides [11, 12, 13, 14, 15]. It has been known that typical DFT correlation functionals are designed for the description of short-range correlations, whereas MP2 is superior to DFTs in the description of

long-range correlations. To handle both types of correlations more appropriately, several double-hybrid DFT methods have been proposed, based on a combination of density functionals for exchange and correlation with Hartree-Fock (HF) exchange and a perturbative second-order correlation obtained from Kohn-Sham orbitals [16, 17, 18]. In particular, the addition of dispersion corrections has shown improved performance of DFTs when predicting the relative conformational energies of neutral amino acids and peptides against the benchmark CCSD(T)/CBS-limit energies [9, 10, 12, 13, 14, 15, 19]. However, no assessment of DFTs has been made for relative conformational energies of charged amino acids or peptides in water, although there was an assessment of DFTs for the clusters of the zwitterionic arginine with halide ion (Cl⁻ and Br⁻) against the benchmark MP2 energies in the gas phase [20].

Nylon-3 polymers (poly-β-peptides) are one of non-natural analogs of host-defense peptides that are produced during the innate immune response to infections by microbes such as bacteria and fungi [21]. In particular, polymers of nylon-3 βNM (Figure 1a) prepared from
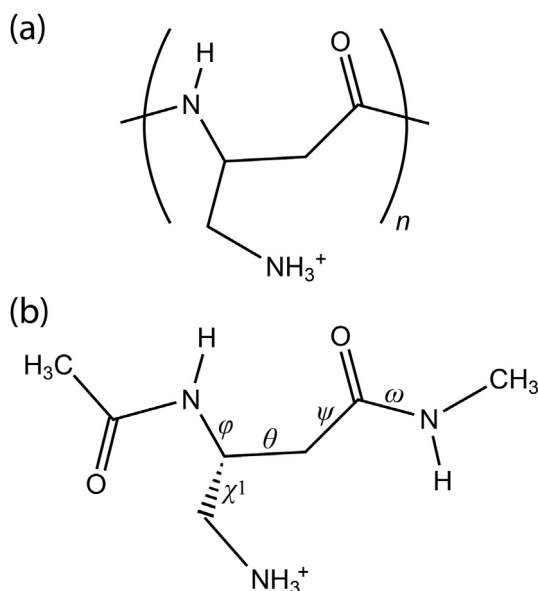
Figure 1. (a) Chemical structure of the cationic βNM (dAba) polymer and (b) chemical structure and torsion angles of the cationic Ac-dAba-NHMe.

β-aminomethyl-β-lactam displayed activity against phylogenetically diverse, intrinsically drug-resistant pathogenic fungi with relatively low toxicity toward mammalian cells [22, 23, 24, 25]. Based upon the membrane leakage experiments by cationic βNM polymers, it was suggested that the ability of cationic polymers to bridge between charged lipid head groups might cause a local depression or invagination of the membrane of fungi [26]. However, conformational preferences of oligomers or polymers for cationic βNM studied in water studied by spectroscopic or computational methods are not available yet.

Here, we explore the conformational preferences of the cationic βNM dipeptide in water as the first step to understand the mode of action of poly-βNM. Dispersion-corrected DFTs were assessed for the relative energies of the 45 local minima of the cationic βNM dipeptide located in water against the benchmark CCSD(T)/CBS-limit energies.

2. Computational methods

Chemical structure and torsional parameters for the cationic βNM [(3R,4)-diaminobutanoic acid, abbreviated as dAba hereafter] dipeptide (Ac-dAba-NHMe) are defined in Figure 1b. The initial structure of the cationic dAba dipeptide with the extended backbone was constructed using the GaussView program [27]. All calculations were carried out using the Gaussian 09 package [28]. All geometry optimizations in water were carried out using the M06-2X functional [29] and the Solvation Model based on Density (SMD) method [30] with the "fine" integration grid that is the default in the Gaussian 09 package. Although the M06-2X functional is a hybrid-meta-GGA functional with the improved medium-range correlation energy, it have been known to exhibit good performance in predicting noncovalent interactions of small molecules and relative stabilities of biological compounds [4]. In particular, the SMD M06-2X/6-31+G(d) level of theory well reproduced solvation free energies of model compounds for the backbone and side chains of peptides in water [31].

Using the extended structure of the neutral and cationic Ac-dAba-NHMe, 1,260 (i.e., 644 and 616 structures for neutral and cationic dipeptides, respectively) initial structures were generated by the systematic search of the Discovery Studio package [32] using the CHARMm force field with the maximum systematic conformations = 1000 and the energy threshold = 20 kcal/mol in the gas phase. In the conformational search, a systematic variation of each of the torsion angles φ, θ, ψ of the backbone and χ^1 of the side chain was done using steps of 60°. The initial

neutral structures were edited by adding protons to produce the cationic species. These 1,260 initial structures were optimized at the SMD HF/3-21G(d) level of theory in water and we obtained 58 local minima with relative energy (ΔE) < 10 kcal/mol, which were reoptimized at the SMD M06-2X/6-31G(d) level of theory in water and further optimized at the SMD M06-2X/6-31+G(d) level of theory in water. Finally, we obtained the 45 local minima for the cationic Ac-dAba-NHMe with ΔE < 5 kcal/mol in water.

Vibrational frequencies were calculated for the 45 local minima for the cationic dAba dipeptide at the SMD M06-2X/6-31+G(d) level of theory in water at 25 °C and 1 atm, of which the scale factor was 0.9440 to reproduce experimental frequency of 1707 cm^{-1} for the amide I band of N-methylacetamide in Ar and N_2 matrixes [33]. The Gibbs free energy of each conformation was calculated from the zero-point energy correction and the thermal energy corrections, from which the populations of all local minima were estimated at 25 °C in water. The translational, rotational, and vibrational contributions to the Gibbs free energy were computed using the ideal gas, rigid rotor, and harmonic oscillator approximations, respectively [34].

Single-point energies (ΔE_{sp}) of the 45 local minima for the cationic dAba dipeptide were calculated at the MP2 level of theory with cc-pVDZ and aug-cc-pVXZ (X = D, T, and Q) basis sets and the CCSD(T) level of theory with the cc-pVDZ basis set. Each CCSD(T)/CBS-limit energy was estimated by the sum of the MP2/CBS-limit energy and the "coupled-cluster correction", ΔCCSD(T). The MP2/CBS-limit energy was obtained using the two-point extrapolation scheme of Halkier et al. [35] with MP2/aug-cc-pVTZ and MP2/aug-cc-pVQZ energies. The value of ΔCCSD(T) was calculated by the difference between CCSD(T) and MP2 energies with the cc-pVDZ basis set. Here, the cc-pVDZ, aug-cc-pVDZ, aug-cc-pVTZ, and aug-cc-pVQZ basis sets are abbreviated as DZ, aDZ, aTZ, and aQZ, respectively.

Then, we assessed the four DFTs classified by rung 4 and rung 5 on the Perdew's "Jacob's Ladder" [36, 37] for relative energies of the 45 local minima for the cationic dAba dipeptide against the benchmark CCSD(T)/CBS-limit energies: two M06-2X [29] and ωB97X-D [38] functionals; and two double-hybrid B2PLYP [39] and DSD-PBEP86 [40] functionals. The basis sets used are cc-pVTZ, def2-TZVP, and def2-QZVP, which are abbreviated as TZ, dTZ, and dQZ, respectively. In particular, the corrections of dispersion were calculated using the Grimme's D3 version with Becke-Johnson damping (i.e., D3BJ) [41] for double-hybrid B2PLYP and DSD-PBEP86 functionals. Recently, the DSD-PBEP86-D3BJ and B2PLYP-D3BJ levels of theory exhibited the best performance against the relative CCSD(T)/CBS-limit energies for the Ala and Pro dipeptides and the Ala tetrapeptide, whereas the M06-2X and ωB97X-D functionals were suggested as an alternative level of theory with marginal deviations [9, 15].

The helix parameters of the H_{14} hexamer were calculated from its six consecutive β-carbons using the HELFIT program [42], based on total least squares algorithm for helix fitting with at least four data points for the analysis.

3. Results and discussion

3.1. Conformational preference of the cationic Ac-dAba-NHMe in water

Torsion angles, relative electronic energies, and solvation free energies of the 45 local minima for the cationic Ac-dAba-NHMe in water located at the CCSD(T)/CBS-limit//SMD M06-2X/6-31+G(d) level of theory are listed in Table 1. For comparison, the conformational codes for Ac-βAbu-NHMe with the –CH$^\beta$(CH$_3$)–CH$_2^\alpha$– backbone obtained at the SCRF HF/6-31G(d) level of theory [43] are shown in parentheses. For C=O···H–N H-bonds, the maximum value of the O···H distance and the minimum value of the O···H–N angle were taken as 2.4 Å and 120°, respectively [44]. There were several types of H-bond for the cationic Ac-dAba-NHMe. C_6 and C_8 are 6- and 8-membered H-bonds for backbone. C_{7a} (or C_{7b}) is the 7-membered H-bond of the H–N$^+$ of the side

Table 1. Torsion angles, relative electronic energies, and solvation free energies of the 45 local minima of the cationic Ac-dAba-NHMe with $\Delta E < 5$ kcal/mol at the CCSD(T)/CBS limit//SMD M06-2X/6-31+G(d) level of theory in water.[a]

Conf.[b]	Type[c]	φ	θ	ψ	χ^1	ΔE_{sp}[d]	ΔG_s[e]	ΔE[f]
m01 (B17^s)	C_{7a}/C_{7b}	70.3	177.9	-105.4	-179.9	0.00	-65.56	0.00
m02 (B10^s)	H_{14}	-162.2	61.7	-137.2	-176.2	13.65	-78.73	0.48
m03 (B10^s)	H_{14}	-142.7	62.9	-140.5	-177.1	19.13	-83.95	0.75
m04	C_6/C_{7a}	-173.3	54.1	102.2	-178.7	10.15	-74.86	0.85
m05	C_{7a}	65.4	59.2	-131.4	-177.9	11.17	-75.87	0.87
m06 (B10^s)	H_{14}	-124.4	60.6	-137.7	-176.6	24.40	-89.07	0.90
m07 (B1^s)	C_6	-143.9	-62.6	-127.7	-177.8	13.43	-77.94	1.05
m08	C_{7b}	-155.2	-171.8	-103.8	179.5	13.18	-77.60	1.15
m09	C_{7b}	-155.8	-53.8	147.6	176.8	8.13	-72.36	1.33
m10 (B3^s)	C_{7b}	-80.0	-75.4	107.3	-179.9	14.64	-78.81	1.39
m11 (B16^s)		-147.8	173.0	131.2	178.0	17.70	-81.71	1.54
m12	C_{7b}	-75.0	155.0	-123.3	-179.0	11.40	-75.42	1.55
m13 (B8^s)	C_{7a}	65.4	167.7	134.8	179.5	12.45	-76.28	1.72
m14 (B9^s)	$H_{10/12}$	-88.6	57.9	91.0	-171.9	28.45	-92.26	1.76
m15	C_{7a}/C_{7b}	76.4	-55.4	92.9	-170.3	5.76	-69.47	1.85
m16 (B16^s)	C_{7a}/C_{7b}	-172.4	173.0	171.3	177.5	3.73	-67.42	1.87
m17 (B10^s)	H_{14}	-155.3	60.9	-133.7	-177.2	28.21	-91.88	1.89
m18 (B6^s)	C_8	-116.7	65.8	10.2	178.9	29.82	-93.45	1.93
m19 (B19^s)	C_{7b}	-151.4	-78.7	111.2	178.8	13.66	-77.27	1.96
m20	C_{7b}	-81.8	-173.7	-99.6	178.4	16.98	-80.55	1.99
m21 (B18^s)	H_{10}	59.7	52.0	86.7	-177.8	14.53	-78.09	2.00
m22 (B3^s)	C_{7b}	-64.4	-38.6	112.6	-177.7	13.15	-76.69	2.02
m23	C_6/C_{7b}	-156.1	-61.8	-179.1	-179.5	8.74	-72.27	2.03
m24 (B1^s)	C_6	-151.8	-63.7	-128.6	-176.8	25.11	-88.62	2.05
m25	H_{14}	-139.0	59.5	-133.9	-179.0	30.24	-93.71	2.09
m26	C_{7a}	-166.0	167.4	-101.1	179.0	11.30	-74.57	2.29
m27		61.8	55.2	-132.0	-179.4	21.36	-84.41	2.51
m28		-160.5	178.2	127.8	177.9	29.49	-92.48	2.57
m29		-142.7	63.2	14.5	179.3	24.23	-87.21	2.59
m30 (B9^s)	$H_{10/12}$	-88.2	56.6	92.0	-173.5	34.15	-96.90	2.81
m31	C_{7b}	68.5	-79.6	123.1	-176.6	12.16	-74.85	2.87
m32	C_{7b}	69.2	164.1	-155.3	-177.5	9.36	-71.87	3.05
m33	C_6	-160.1	58.3	103.0	-179.8	26.80	-89.30	3.06
m34	C_6	-165.3	58.3	98.5	-177.2	22.58	-85.02	3.13
m35 (B6^s)	C_8	-113.8	62.7	17.1	179.1	32.43	-94.71	3.28
m36		63.6	168.5	128.6	178.7	22.63	-84.91	3.29
m37		-77.6	170.6	125.2	179.6	38.00	-100.08	3.49
m38 (B6^s)	C_8	-114.3	69.5	6.2	-179.6	34.62	-96.67	3.51
m39		67.5	56.3	-133.2	-178.6	25.05	-87.09	3.52
m40 (B18^s)	H_{10}	59.1	48.9	85.6	-176.6	27.14	-89.14	3.56
m41 (B3'^{s})		56.4	47.0	-113.5	177.3	25.99	-87.88	3.67
m42		-149.9	66.6	7.6	179.9	32.27	-94.06	3.78
m43	C_{7a}	79.6	-57.6	93.2	-169.9	21.63	-83.29	3.90
m44 (B2^s)	C_8	-71.4	139.7	-74.8	175.0	29.88	-91.32	4.12
m45 (B12^s)	C_{7a}	-173.7	-70.7	18.4	178.4	20.43	-81.22	4.77

[a] Units for torsion angles, relative electronic energies, and solvation free energies in degrees, kcal/mol, and kcal/mol, respectively. Torsion angles are defined in Figure 1b. All local minima were optimized at the SMD M06-2X/6-31+G(d) level of theory in water.
[b] The conformation in parentheses were for Ac-βAbu-NHMe from Table V of Ref. [43].
[c] Conformation types. C_6 and C_8 are 6- and 8-membered H-bonds for backbone. C_{7a} and C_{7b} are 7-membered H-bonds between the C=O of the acetyl group and the H–N$^+$ of the side chain and between the C=O of the dAba residue and the H–N$^+$ of the side chain, respectively. H_n is the monomer of helix with n-membered H-bonded turn available for oligomers beyond the monomer or dimer.
[d] The relative CCSD(T)/CBS limit single-point energies.
[e] Solvation free energies were calculated at the SMD M06-2X/6-31+G(d) level of theory in water.
[f] Each relative energy in water was calculated by the sum of the ΔE_{sp} and ΔG_s energies.

chain of the dAba residue with the C=O of the acetyl group (or the dAba residue). H_{14}, $H_{10/12}$, and H_{10} are the monomer of helices with 14-, 10/12-, and 10-membered H-bonded turns, respectively, which are available for oligomers beyond the monomer or dimer (see Ref. [43]).

Absolute and relative thermodynamic properties and solvation free energies of the 45 local minima of the cationic Ac-dAba-NHMe with $\Delta E < 5$ kcal/mol optimized at the SMD M06-2X/6-31+G(d) level of theory in water are listed in Table S1 of the Supplementary material. In addition,
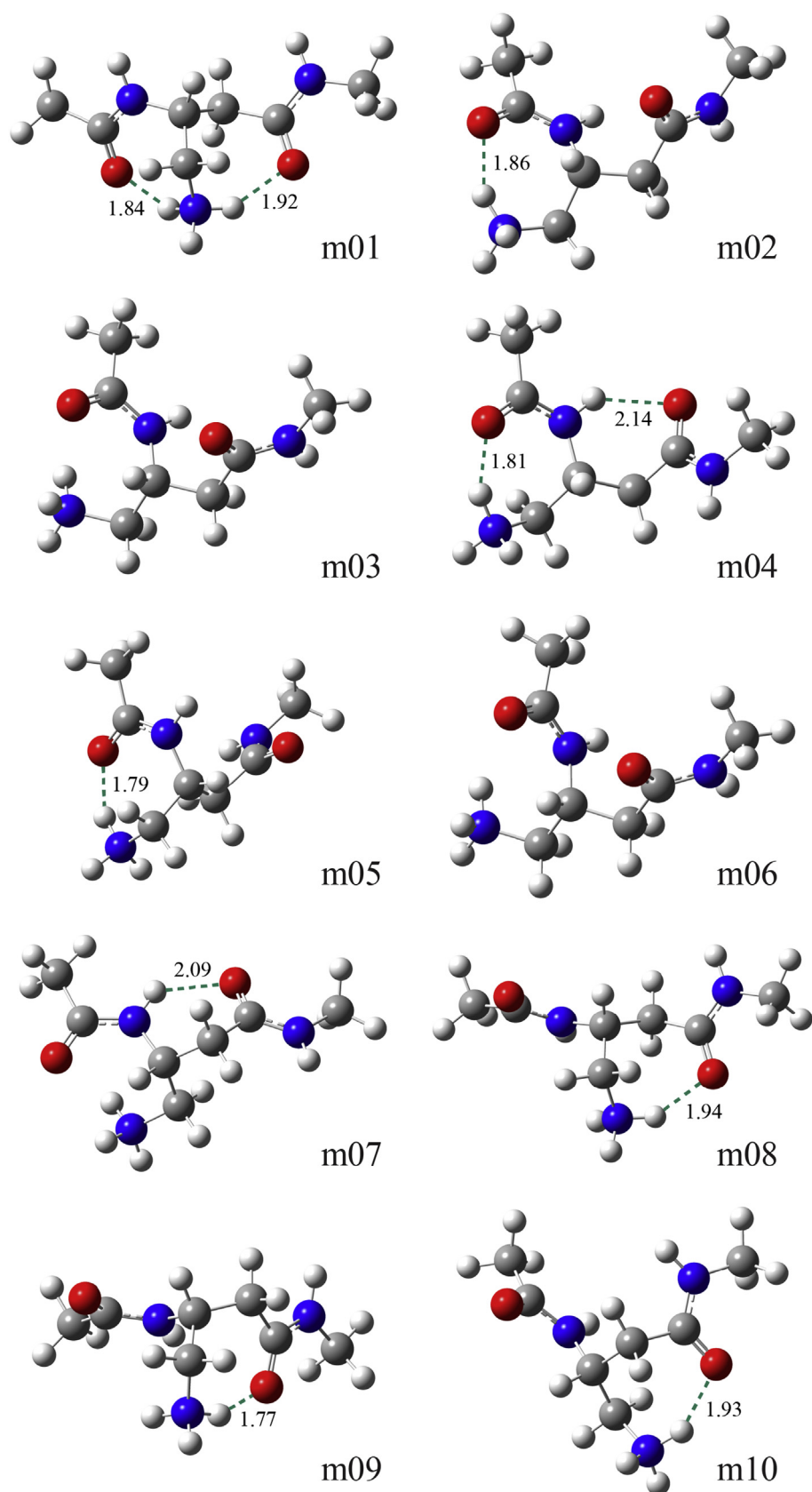
Figure 2. Structures of the first ten lowest-energy conformations for the cationic Ac-dAba-NHMe with $\Delta E < 1.50$ kcal/mol in water obtained at the CCSD(T)/CBS limit//SMD M06-2X/6-31+G(d) level of theory. H-bonds are represented by dotted lines and their distances are in Å.

Table 2. Relative energies (kcal/mol) of the 45 local minima of the cationic Ac-dAba-NHMe in water.[a]

Conf.	CCSD(T)		MP2					M06-2X			ωB97X-D			B2PLYP-D3BJ			DSD-PBEP86-D3BJ		
	CBS	DZ	DZ	aDZ	aTZ	aQZ	CBS	TZ	dTZ	dQZ	TZ	dTZ	dQZ	TZ	dTZ	dQZ	TZ	dTZ	dQZ
m01	0.00	0.00	0.00	0.00	0.00	0.00	0.00	0.00	0.00	0.00	0.00	0.00	0.00	0.00	0.00	0.00	0.00	0.00	0.00
m02	0.48	1.21	1.18	0.39	0.45	0.45	0.45	1.35	1.15	1.09	1.23	0.96	0.86	0.80	0.49	0.49	0.77	0.47	0.52
m03	0.75	1.93	1.56	0.04	0.28	0.34	0.38	1.29	0.93	1.00	1.90	1.43	1.41	1.56	0.92	1.08	1.24	0.54	0.82
m04	0.85	1.68	1.73	1.01	0.94	0.91	0.90	1.66	1.50	1.41	1.59	1.37	1.28	1.23	0.98	0.94	1.22	0.99	0.95
m05	0.87	1.30	1.26	0.40	0.64	0.75	0.83	1.26	1.10	1.14	1.12	0.87	0.90	1.06	0.73	0.86	1.03	0.68	0.88
m06	0.90	1.67	1.17	0.02	0.23	0.32	0.39	1.82	1.37	1.53	2.07	1.52	1.54	1.61	0.93	1.13	1.31	0.57	0.90
m07	1.05	2.19	1.90	0.57	0.68	0.72	0.76	1.24	0.90	1.04	1.94	1.51	1.59	1.81	1.26	1.42	1.50	0.88	1.15
m08	1.15	1.92	1.67	0.79	0.91	0.90	0.90	1.38	1.17	1.19	1.81	1.56	1.49	1.63	1.33	1.36	1.40	1.09	1.18
m09	1.33	1.77	1.68	1.21	1.16	1.21	1.25	1.57	1.33	1.44	1.52	1.25	1.31	1.58	1.25	1.37	1.49	1.14	1.32
m10	1.39	2.06	1.83	1.00	1.06	1.12	1.16	1.62	1.40	1.47	1.83	1.57	1.57	1.74	1.42	1.51	1.55	1.21	1.36
m11	1.54	3.17	2.87	1.04	1.20	1.22	1.24	1.87	1.41	1.50	2.62	2.06	2.05	2.48	1.77	1.90	2.12	1.34	1.61
m12	1.55	2.78	2.91	1.81	1.72	1.70	1.68	2.40	2.12	2.01	2.11	1.78	1.66	2.01	1.65	1.54	2.02	1.68	1.58
m13	1.72	2.06	2.00	1.35	1.58	1.63	1.66	1.77	1.72	1.72	1.56	1.45	1.40	1.73	1.59	1.63	1.73	1.56	1.67
m14	1.76	2.34	2.00	0.39	1.06	1.27	1.42	2.26	2.00	2.16	3.11	2.71	2.73	2.56	2.00	2.23	2.21	1.59	1.94
m15	1.85	1.02	0.77	0.45	1.09	1.39	1.60	1.18	1.34	1.48	1.47	1.65	1.76	1.54	1.66	1.85	1.54	1.60	1.82
m16	1.87	2.50	2.71	2.04	2.09	2.08	2.08	1.28	1.04	1.17	3.11	2.74	2.83	2.98	2.53	2.65	2.55	2.07	2.27
m17	1.89	2.81	2.59	1.33	1.61	1.65	1.68	2.97	2.62	2.59	3.18	2.67	2.58	2.66	2.06	2.12	2.42	1.80	1.98
m18	1.93	3.23	2.74	0.84	1.10	1.30	1.44	2.66	2.27	2.37	2.86	2.37	2.40	2.62	2.03	2.20	2.32	1.72	1.95
m19	1.96	2.14	1.93	1.61	1.70	1.73	1.75	2.04	1.89	1.98	2.35	2.13	2.15	2.20	1.96	2.06	2.02	1.76	1.93
m20	1.99	2.64	2.52	1.73	1.88	1.87	1.87	2.28	2.06	2.05	2.47	2.21	2.14	2.37	2.06	2.06	2.25	1.93	1.99
m21	2.00	1.89	1.91	1.30	1.74	1.90	2.02	2.20	2.18	2.21	2.08	1.96	1.97	2.06	1.85	2.00	2.04	1.79	2.01
m22	2.02	2.32	2.24	1.20	1.62	1.81	1.94	2.11	2.03	2.16	2.09	1.92	2.05	2.03	1.77	1.99	2.02	1.72	2.03
m23	2.03	2.19	2.12	1.88	1.88	1.92	1.96	1.78	1.65	1.82	2.10	1.93	2.03	2.22	2.00	2.18	2.07	1.80	2.06
m24	2.05	2.91	2.72	1.67	1.79	1.83	1.86	2.69	2.35	2.41	3.01	2.56	2.56	2.73	2.21	2.30	2.52	1.97	2.15
m25	2.09	2.72	2.42	1.44	1.71	1.76	1.79	3.26	2.88	2.90	3.25	2.75	2.67	2.76	2.15	2.26	2.54	1.90	2.14
m26	2.29	3.13	3.19	2.56	2.46	2.40	2.35	2.98	2.77	2.70	2.82	2.56	2.46	2.68	2.41	2.34	2.66	2.41	2.36
m27	2.51	3.50	3.22	1.67	2.05	2.15	2.23	2.95	2.55	2.83	3.52	3.00	3.15	3.24	2.57	2.90	2.92	2.17	2.66
m28	2.57	3.72	3.29	1.77	2.02	2.09	2.14	3.07	2.73	2.79	3.47	3.06	2.96	3.28	2.77	2.86	2.94	2.39	2.61
m29	2.59	4.29	3.93	1.63	1.92	2.10	2.23	2.91	2.48	2.62	3.39	2.85	2.89	3.38	2.70	2.87	3.05	2.31	2.60
m30	2.81	3.41	3.27	1.68	2.33	2.53	2.67	3.39	3.18	3.22	4.18	3.79	3.75	3.56	3.05	3.18	3.33	2.76	3.02
m31	2.87	2.59	2.51	2.20	2.56	2.69	2.79	2.59	2.62	2.73	3.50	3.48	3.57	3.08	3.01	3.16	2.93	2.82	3.02
m32	3.05	3.44	3.83	3.32	3.51	3.47	3.44	3.04	2.83	2.89	3.71	3.42	3.44	3.69	3.38	3.39	3.56	3.24	3.30
m33	3.06	4.15	4.08	2.76	2.97	2.98	2.99	3.96	3.68	3.62	4.34	3.89	3.79	3.86	3.33	3.32	3.68	3.13	3.22
m34	3.13	3.67	3.32	2.46	2.72	2.76	2.78	3.65	3.37	3.53	4.02	3.66	3.70	3.69	3.23	3.42	3.41	2.91	3.20
m35	3.28	4.20	3.93	2.45	2.72	2.89	3.01	4.23	3.95	3.91	4.22	3.82	3.78	3.88	3.42	3.50	3.69	3.22	3.36
m36	3.29	4.61	4.39	2.68	3.01	3.04	3.07	3.71	3.23	3.43	4.25	3.68	3.74	4.19	3.48	3.70	3.85	3.07	3.44
m37	3.49	4.53	4.21	2.76	3.08	3.13	3.17	4.14	3.90	3.75	4.42	4.09	3.84	4.15	3.74	3.64	3.96	3.52	3.53
m38	3.51	4.52	4.25	2.61	2.88	3.09	3.24	4.30	4.04	3.95	4.30	3.93	3.84	4.08	3.63	3.65	3.92	3.48	3.56
m39	3.52	4.26	4.29	2.92	3.39	3.48	3.54	4.01	3.73	3.84	4.45	4.00	4.05	4.22	3.65	3.84	4.00	3.37	3.70
m40	3.56	3.94	3.65	2.46	2.98	3.15	3.27	3.92	3.63	3.87	4.62	4.21	4.31	4.25	3.69	4.01	3.90	3.26	3.72
m41	3.67	4.12	3.94	2.44	3.18	3.36	3.49	3.86	3.61	3.86	4.42	3.96	4.13	4.29	3.67	4.05	3.99	3.29	3.83
m42	3.78	4.91	4.52	2.75	3.10	3.26	3.38	4.32	3.94	4.04	4.44	3.95	3.93	4.42	3.84	3.97	4.12	3.51	3.75
m43	3.90	3.61	3.00	1.54	2.56	2.98	3.29	3.13	3.12	3.33	4.87	4.73	4.88	4.52	4.28	4.56	3.97	3.65	4.03
m44	4.12	5.00	4.83	3.41	3.71	3.85	3.94	4.63	4.29	4.43	5.11	4.60	4.63	4.97	4.35	4.50	4.68	4.01	4.28
m45	4.77	4.89	4.82	4.21	4.37	4.56	4.70	4.75	4.60	4.69	5.04	4.83	4.84	5.03	4.78	4.91	4.84	4.59	4.77
RMSD[b]		0.85	0.71	0.79	0.46	0.34	0.27	0.58	0.39	0.38	0.85	0.50	0.51	0.61	0.19	0.29	0.39	0.19	0.12

[a] All structures were optimized at the SMD M06-2X/6-31+G(d) level of theory in water. Each relative energy was calculated by the sum of the single-point energy (ΔE_{sp}) and the solvation free energy (ΔG_s) as in Table 1. The CBS limit, cc-pVDZ, cc-pVTZ, aug-cc-pVDZ, aug-cc-pVTZ, aug-cc-pVQZ, def2-TZVP, and def2-QZVP basis sets are abbreviated as CBS, DZ, TZ, aDZ, aTZ, aQZ, dTZ, and dQZ, respectively.

[b] RMSD against the values obtained at the CCSD(T)/CBS limit level of theory.

absolute and relative single-point energies of the same 45 local minima calculated by M06-2X, ωB97X-D, B2PLYP-D3BJ, DSD-PBEP86-D3BJ, MP2, and CCSD(T) methods are shown in Tables S2–S5 of the Supplementary material. Cartesian coordinates of the 45 local minima optimized at the SMD M06-2X/6-31+G(d) level of theory in water are also listed in Table S6 of the Supplementary material.

The optimized structures of the first ten lowest-energy conformers (m01−m10) with $\Delta E < 1.5$ kcal/mol in water at the CCSD(T)/CBS-limit//SMD M06-2X/6-31+G(d) level of theory are shown in Figure 2. The lowest-energy conformer m01 was stabilized by a bifurcated H-bond of the H–N$^+$ group of the side chain with two C=O groups of the backbone with d(C=O⋯H–N$^+$) = 1.84 and 1.92 Å for C_{7a} and C_{7b} H-bonds, respectively. The second and third lowest-energy conformers (m02 and
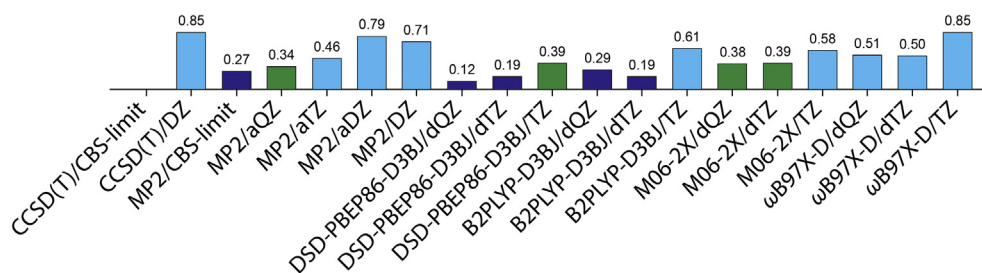
Figure 3. RMSDs (kcal/mol) for relative energies (ΔE) of the 45 local minima of the cationic Ac-dAba-NHMe in water obtained at the CCSD(T), MP2, DSD-PBEP86-D3BJ, B2PLYP-D3BJ, M06-2X, and ωB97X-D levels of theory with various basis sets against the benchmark CCSD(T)/CBS-limit energies. Dark blue histograms for RMSD <0.3 kcal/mol; dark green histograms for 0.3 kcal/mol $\leq$ RMSD $\leq$0.4 kcal/mol; light blue histograms for RMSD >0.4 kcal/mol.

m03) adopted the H_{14} conformation similar to the monomer of a helix with 14-membered H-bonded turns. Although conformers m02 and m03 had similar relative energies ($\Delta E = 0.48$ and 0.75 kcal/mol, respectively), the former had the favored single-point energy (ΔE_{sp}) by 5.48 kcal/mol but the disfavored solvation energy (ΔG_s) by 5.22 kcal/mol than the latter. This seemed to be due to the formation of a C_{7a} H-bond for the former between the acetyl C=O group and the cationic H–N$^+$ group of the side chain with $d(C=O \cdots H-N^+) = 1.86$ Å, whereas the latter had the favored solvation due to the longer distance between C_{7a} H-bond partners with $d(C=O \cdots H-N^+) = 2.59$ Å.

Although the following three lowest-energy conformers (m04, m05, and m06) had comparable conformational energies (0.85, 0.87, and 0.90 kcal/mol, respectively), they had different patterns of conformational features. Conformer m04 was stabilized by a C_6 H-bond between the N–H group and the C=O group of the dAba residue with $d(C=O \cdots H-N) = 2.14$ Å and a C_{7a} H-bond with $d(C=O \cdots H-N^+) = 1.81$ Å. Conformer m05 was stabilized by a short C_{7a} H-bond with $d(C=O \cdots H-N^+) = 1.79$ Å. Although conformer m06 adopted a H_{14} conformation similar to conformer m02 and m03, the former was 10.75 and 5.27 kcal/mol less favored in ΔE_{sp} but -10.34 and -5.12 kcal/mol more favored in ΔG_s than the latter, respectively.

The ΔE values of the next four lowest-energy conformers (m07$-$m10) were 1.05–1.39 kcal/mol, in which conformer m07 had a C_6 H-bond with the distance of $d(C=O \cdots H-N) = 2.09$ Å, whereas conformers m08$-$m10 had a C_{7b} H-bond with $d(C=O \cdots H-N^+) = 1.94, 1.77$, and 1.93 Å, respectively. In particular, conformers m15 and m16 with a bifurcated H-bond with C_{7a} and C_{7b} types of H-bonds, as in the lowest-energy conformer m01, had the third and second lowest value of $\Delta E_{sp} = 5.76$ and 3.73 kcal/mol, respectively, but its ΔE value was 1.85 and 1.87 kcal/mol in water, respectively, due to the less favored solvation. There were 10 local minima for 1.5 kcal/mol < ΔE < 2.0 kcal/mol; 11 local minima for 2.0 kcal/mol $\leq \Delta E$ < 3.0 kcal/mol; 14 local minima for 3.0 kcal/mol < ΔE < 5.0 kcal/mol.

Möhle et al. explored the conformational preference of Ac-βAbu-NHMe at the SCRF HF/6-31G(d) level of theory in water [43]. The authors found the energetic stability of three representative conformers was in the order B1^s > B10^s > B17^s with $\Delta E = 0.00, 2.10$, and 4.25 kcal/mol in water, respectively. Conformer B1^s, B10^s, and B17^s correspond to conformer m07, m02/m03, and m01 in this work, respectively (see Table 1). However, the conformational preference for the cationic Ac-dAba-NHMe were calculated as in the order m01 > m02 > m03 > m07 with $\Delta E = 0.00, 0.48, 0.75$, and 1.05 kcal/mol in water, respectively, at the SMD M06-2X/6-31+G(d) level of theory. As described above, conformer m01 had a bifurcated H-bond of the H–N$^+$ group of the side chain with two C=O groups of the backbone, conformer m02 and m03 adopted a H_{14}-type structure, and conformer m07 had a C_6 H-bond. The different conformational preference of the cationic Ac-dAba-NHMe from that of Ac-βAbu-NHMe can be ascribed to the formation of stronger H-bonds or favored electrostatic interactions between the C=O

groups of the backbone and the H–N$^+$ group of the side chain than the C_6 H-bond between the N–H group and the C=O group of the dAba residue (see Figure 2).

3.2. Assessments for conformational energies in water

The relative conformational energies (ΔE) in water and their RMSDs of the 45 local minima for the cationic Ac-dAba-NHMe at the CCSD(T), MP2, M06-2X, ωB97X-D, B2PLYP-D3BJ, and DSD-PBEP86-D3BJ levels of theory with various basis sets against the benchmark energies obtained by the sum of CCSD(T)/CBS-limit energies and solvation free energies are listed in Table 2. The ΔE value spanned up to 4.77 kcal/mol (conformer m45) at the CCSD(T)/CBS-limit//SMD M06-2X/6-31+G(d) level of theory in water. The RMSDs of ΔE values for the 45 local minima for the cationic Ac-dAba-NHMe in water at various levels of theory are depicted in Figure 3. In particular, the conformer m01 with a bifurcated H-bond (i.e., having C_{7a} and C_{7b} H-bonds) of the H–N$^+$ group of the side chain with two C=O groups of the backbone was identified as the lowest-energy structure in water at all the levels of theory considered in this work.

The double-hybrid DSD-PBEP86-D3BJ/dQZ level of theory exhibited the best performance (RMSD = 0.12 kcal/mol) against the benchmark CCSD(T)/CBS-limit energies in water and was followed by the several levels of theory with small RMSD values in the order DSD-PBEP86-D3BJ/dTZ (0.19) = B2PLYP-D3BJ/dTZ (0.19) > MP2/CBS-limit (0.27) $\approx$ B2PLYP-D3BJ/dQZ (0.29), where RMSD values are in parentheses. In particular, the DSD-PBEP86-D3BJ/dQZ level of theory well predicted the order of conformational stability at the CCSD(T)/CBS-limit level of theory in water, except for the relative stabilities of conformer m04, m14, and m16 with marginal deviations.

The M06-2X/dQZ and M06-2X/dTZ levels of theory exhibited a better performance (RMSD = 0.38 and 0.39 kcal/mol, respectively) than the MP2/aTZ level of theory (RMSD = 0.46 kcal/mol) and the B2PLYP-D3BJ/TZ level of theory (RMSD = 0.61 kcal/mol), which are similar to those of the MP2/aQZ and DSD-PBEP86-D3BJ/TZ levels of theory (RMSD = 0.34 and 0.39 kcal/mol, respectively). However, the CCSD(T)/DZ, MP2/aDZ, and MP2/DZ levels of theory exhibited a little worse performance (RMSD = 0.85, 0.79, and 0.71 kcal/mol, respectively). The M06-2X/TZ, ωB97X-D/dQZ, ωB97X-D/dTZ, and ωB97X-D/TZ levels of theory exhibited the performance with RMSD = 0.58, 0.51, 0.50, and 0.85 kcal/mol, respectively.

Hence, the double-hybrid DSD-PBEP86-D3BJ/def2-QZVP level of theory is expected to provide the accurate relative conformational energies of the peptide with cationic side chains with RMSD $\approx$0.1 kcal/mol in water comparable to the benchmark CCSD(T)/CBS-limit energies. In particular, the M06-2X/dQZ level of theory exhibited a good performance (RMSD <0.4 kcal/mol) against the benchmark energies and may be an alternative level of theory with marginal deviations for the calculation of conformational energies of the larger cationic peptides in water.

Table 3. Free energies (kcal/mol) and populations (%) of the 45 local minima of the cationic Ac-dAba-NHMe in water.[a]

| Conf. | CCSD(T) | | DSD-PBEP86-D3BJ | | | | M06-2X | |
| | CBS limit | | def2-QZVP | | def2-TZVP | | def2-QZVP | |
	ΔG	w	ΔG	w	ΔG	w	ΔG	w
m02	0.00	40.0	0.00	40.7	0.00	33.8	0.00	24.9
m03	0.52	16.5	0.57	15.7	0.34	19.1	0.18	18.5
m06	1.03	7.1	1.00	7.6	0.72	10.0	1.05	4.2
m09	1.41	3.7	1.37	4.1	1.24	4.2	0.91	5.3
m23	1.45	3.4	1.45	3.5	1.25	4.1	0.64	8.5
m12	1.46	3.4	1.45	3.5	1.60	2.3	1.31	2.7
m05	1.48	3.3	1.46	3.5	1.31	3.7	1.14	3.6
m07	1.48	3.3	1.54	3.0	1.33	3.6	0.87	5.8
m01	1.55	2.9	1.51	3.2	1.57	2.4	0.94	5.1
m04	1.64	2.5	1.70	2.3	1.79	1.7	1.59	1.7
m11	1.64	2.5	1.68	2.4	1.46	2.9	0.99	4.7
m14	1.72	2.2	1.87	1.7	1.57	2.4	1.52	1.9
m19	1.93	1.6	1.87	1.7	1.75	1.8	1.35	2.5
m17	2.21	1.0	2.26	0.9	2.13	0.9	2.30	0.5
m08	2.36	0.7	2.35	0.8	2.31	0.7	1.79	1.2
m27	2.41	0.7	2.53	0.6	2.09	1.0	2.13	0.7
m28	2.51	0.6	2.51	0.6	2.34	0.6	2.12	0.7
m29	2.65	0.5	2.63	0.5	2.39	0.6	2.08	0.7
m26	2.71	0.4	2.74	0.4	2.85	0.3	2.52	0.4
m10	2.72	0.4	2.66	0.5	2.56	0.4	2.20	0.6
m16	2.77	0.4	3.13	0.2	2.99	0.2	1.46	2.1
m22	2.89	0.3	2.86	0.3	2.61	0.4	2.43	0.4
m21	2.93	0.3	2.90	0.3	2.74	0.3	2.53	0.3
m24	2.97	0.3	3.04	0.2	2.90	0.3	2.73	0.3
m15	2.98	0.3	2.92	0.3	2.75	0.3	2.01	0.8
m25	3.00	0.3	3.01	0.3	2.83	0.3	3.20	0.1
m18	3.04	0.2	3.02	0.2	2.84	0.3	2.87	0.2
m38	3.08	0.2	3.10	0.2	3.07	0.2	2.92	0.2
m40	3.09	0.2	3.22	0.2	2.81	0.3	2.80	0.2
m30	3.21	0.2	3.38	0.1	3.18	0.2	3.01	0.2
m36	3.39	0.1	3.50	0.1	3.18	0.2	2.93	0.2
m32	3.62	0.1	3.83	0.1	3.82	0.1	2.85	0.2
m13	3.69	0.1	3.60	0.1	3.54	0.1	3.08	0.1
m39	3.75	0.1	3.90	0.1	3.62	0.1	3.47	0.1
m20	3.82	0.1	3.78	0.1	3.78	0.1	3.28	0.1
m33	4.09	0.0	4.21	0.0	4.18	0.0	4.04	0.0
m31	4.11	0.0	4.22	0.0	4.08	0.0	3.36	0.1
m41	4.14	0.0	4.26	0.0	3.78	0.1	3.72	0.0
m34	4.23	0.0	4.27	0.0	4.03	0.0	4.03	0.0
m37	4.29	0.0	4.29	0.0	4.33	0.0	3.94	0.0
m35	4.37	0.0	4.41	0.0	4.32	0.0	4.39	0.0
m44	4.38	0.0	4.51	0.0	4.29	0.0	4.09	0.0
m42	4.60	0.0	4.54	0.0	4.35	0.0	4.26	0.0
m43	5.99	0.0	6.09	0.0	5.75	0.0	4.82	0.0
m45	6.73	0.0	6.70	0.0	6.56	0.0	6.04	0.0

[a] All structures were optimized at the SMD M06-2X/6-31+G(d) level of theory in water. Each relative Gibbs free energy (ΔG) was calculated by the sum of ΔE (Table 2) and the enthalpic and entropic contributions (i.e., ΔH_c and $-T\Delta S_c$ in Table S1 of the Supplementary material).

3.3. Conformational free energies in water

The relative Gibbs free energies (ΔG) and populations of the 45 local minima for the cationic Ac-dAba-NHMe in water using single-point energies at the CCSD(T)/CBS-limit, DSD-PBEP86-D3BJ (with dQZ and dTZ basis sets), and M06-2X/dQZ levels of theory are listed in Table 3. Conformer m02 with a H_{14}–helix backbone was identified as the most preferred conformation in water at all the CCSD(T)/CBS-limit, DSD-PBEP86-D3BJ/dQZ, DSD-PBEP86-D3BJ/dTZ, and M06-2X/dQZ levels of

theory (populated at 40, 41, 34, and 25%, respectively). The second most preferred conformer m03 also adopted a H_{14}–helix backbone at the same levels of theory (populated at 17, 16, 19, and 19%, respectively). However, the third most preferred conformation was m06 with a H_{14}–helix backbone at the first three levels of theory (populated at 7, 8, and 10%, respectively), whereas the corresponding conformation was m23 with C_6/C_{7b} H-bonds with a population of 9% and conformer m06 was populated at 4% at the M06-2X/dQZ level of theory. Hence, the H_{14}–structure appeared to be the most feasible conformation for the
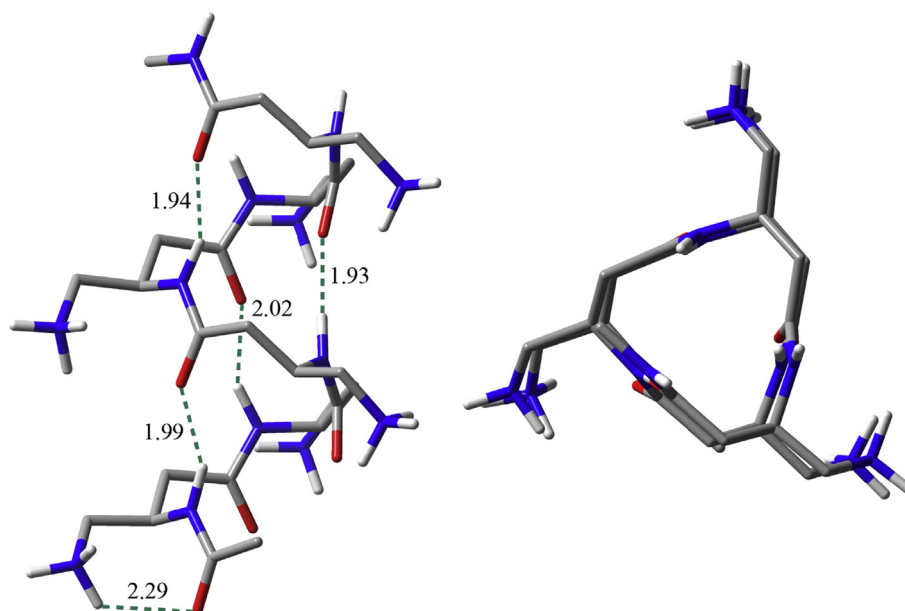
Figure 4. Structure of the hexamer from conformer m03 of the cationic Ac-dAba-NHMe in water optimized at the SMD M06-2X/6-31G(d) level of theory: (left) view along the helix axis and (right) view perpendicular to the helical axis. H-bonds are represented by dotted lines and their distances are in Å.

cationic Ac-dAba-NHMe in water populated at 48–64% at all the levels of theory considered in this work.

As described in earlier section, conformer m01 was the lowest-energy structure at all the levels of theory. However, its free energy was 1.55, 1.51, 1.57, and 0.94 kcal/mol at the CCSD(T)/CBS-limit, DSD-PBEP86-D3BJ/dQZ, DSD-PBEP86-D3BJ/dTZ, and M06-2X/dQZ levels of theory, respectively. The increased ΔG value for m01 was ascribed to the decrease of the entropic contribution (see Table S1 of the Supplementary material), i.e., the less conformational flexibility due to the formation of a bifurcated H-bond with C_{7a} and C_{7b} H-bonds (see Figure 2).

From the two most preferred conformers m02 and m03 in water, two hexamers of the cationic Ac-dAba-NHMe were built and optimized at the SMD M06-2X/6-31G(d) level of theory in water. Two optimized structures were quite similar to each other but the hexamer from conformer m03 was 0.52 kcal/mol more stable than that from conformer m02. The optimized structure of the hexamer from conformer 03 is depicted in Figure 4 and its Cartesian coordinates is listed in Table S7 of the Supplementary material. The hexamer adopted a left-handed 3_{14}-helix with radius = 2.57 Å, residues/turn = 3.0, and rise/residue = 1.71 Å. This 3_{14}-helix has a slightly narrower radius and a longer rise than the regular 3_{14}-helix of β-peptides with radius = 2.7 Å and rise/residue = 1.56 Å [45]. The mean backbone torsion angles for the 3_{14}-helix of the hexamer from conformer m03 are $\varphi = -132°$, $\theta = 58°$, and $\psi = -139°$, whereas those are $\varphi = -150°$, $\theta = 62°$, and $\psi = -138°$ for the H_{14}-helix of the tetramer of βAbu optimized at the HF/6-31G(d) level of theory [43]. We monitored the H-bond distances $d(C{=}O{\cdots}H{-}N)$ for the 3_{14}-helix of the hexamer of conformer m03, whose mean value is 1.97 Å for backbone and the distance for the first C_{7a} H-bond is 2.29 Å (see Figure 4). Hence, the 3_{14}-helices of oligomers or polymers of the cationic dAba residues are expected to be the active conformation to exhibit the ability to bridge between charged lipid head groups that might cause a local depression or invagination of the membrane of fungi, suggested from the membrane leakage experiments [26].

4. Conclusions

We explored the conformational preferences of the cationic nylon-3 βNM (dAba) dipeptide in water as the first step to understand the mode of action of polymers of βNM against phylogenetically diverse and intrinsically drug-resistant pathogenic fungi. At the SMD M06-2X/6-

31+G(d) level of theory in water, the 45 local minima of the cationic Ac-dAba-NHMe with $\Delta E < 5$ kcal/mol were identified. The CCSD(T), MP2, M06-2X, ωB97X-D, B2PLYP-D3BJ, and DSD-PBEP86-D3BJ levels of theory with various basis sets were assessed for relative energies of these 45 local minima against the benchmark CCSD(T)/CBS-limit energies in water.

The double-hybrid DSD-PBEP86-D3BJ/def2-QZVP level of theory exhibited the best performance (RMSD = 0.12 kcal/mol) in water against to the benchmark CCSD(T)/CBS-limit energies and was followed by the several levels of theory such as DSD-PBEP86-D3BJ/def2-TZVP, B2PLYP-D3BJ/def2-TZVP, MP2/CBS-limit, and B2PLYP-D3BJ/def2-QZVP with small RMSD values (0.19–0.29 kcal/mol). In particular, the DSD-PBEP86-D3BJ/def2-QZVP level of theory well predicted the order of conformational stability at the CCSD(T)/CBS-limit level of theory in water. The M06-2X/dQZ and M06-2X/dTZ levels of theory exhibited a better performance (RMSD = 0.38 and 0.39 kcal/mol, respectively) than the MP2/aTZ and B2PLYP-D3BJ/TZ levels of theory. Hence, the M06-2X/def2-QZVP level of theory may be an alternative level of theory with marginal deviations to reduce the computational times without any significant loss in accuracy for conformational energies of relatively longer cationic peptides in water.

In particular, the H_{14}–helical structures appeared to be the most feasible conformations for the cationic Ac-dAba-NHMe populated at 48–64% by relative free energies in water. The hexamer built from the H_{14}–structure of the cationic Ac-dAba-NHMe adopted a left-handed 3_{14}-helix, which has a slightly narrower radius and a longer rise than the regular 3_{14}-helix of β-peptides. Hence, the 3_{14}-helices of oligomers or polymers of the cationic dAba residues are expected to be the active conformation to exhibit the ability to bridge between charged lipid head groups that might cause a local depression or invagination of the membrane of fungi.

Declarations

Author contribution statement

Young Kee Kang: Conceived and designed the analysis; Analyzed and interpreted the data; Contributed analysis tools or data; Wrote the paper.

Hae Sook Park: Analyzed and interpreted the data; Contributed analysis tools or data; Wrote the paper.

Competing interest statement

The authors declare no conflict of interest.

Additional information

Supplementary content related to this article has been published online at https://doi.org/10.1016/j.heliyon.2020.e04721.

References

[1] A.G. Császár, A. Perczel, Ab initio characterization of building units in peptides and proteins, Prog. Biophys. Mol. Biol. 71 (1999) 243–309.

[2] K.J. Jalkanen, M. Elstner, S. Suhai, Amino acids and small peptides as building blocks for proteins: comparative theoretical and spectroscopic studies, J. Mol. Struct. Theochem. 675 (2004) 61–77.

[3] K.E. Riley, M. Pitoňák, P. Jurečka, P. Hobza, Stabilization and structure calculations for noncovalent interactions in extended molecular systems based on wave function and density functional theories, Chem. Rev. 110 (2010) 5023–5063.

[4] Y. Zhao, D.G. Truhlar, Applications and validations of the Minnesota density functionals, Chem. Phys. Lett. 502 (2011) 1–13.

[5] S. Grimme, A. Hansen, J.G. Brandenburg, C. Bannwarth, Dispersion-corrected mean-field electronic structure methods, Chem. Rev. 116 (2016) 5105–5154.

[6] L. Goerigk, A. Hansen, C. Bauer, S. Ehrlich, A. Najibi, S. Grimme, A look at the density functional theory zoo with the advanced GMTKN55 database for general main group thermochemistry, kinetics and noncovalent interactions, Phys. Chem. Chem. Phys. 19 (2017) 32184–32215.

[7] K.A. Peterson, D. Feller, D.A. Dixon, Chemical accuracy in ab initio thermochemistry and spectroscopy: current strategies and future challenges, Theor. Chem. Acc. 131 (2012) 1079.

[8] J.J. Wilke, M.C. Lind, H.F. Schaefer III, A.G. Császár, W.D. Allen, Conformers of gaseous cysteine, J. Chem. Theor. Comput. 5 (2009) 1511–1523.

[9] Y.K. Kang, H.S. Park, Assessment of CCSD(T), MP2, DFT-D, CBS-QB3, and G4(MP2) methods for conformational study of alanine and proline dipeptides, Chem. Phys. Lett. 600 (2014) 112–117.

[10] M.K. Kesharwani, A. Karton, J.M.L. Martin, Benchmark *ab initio* conformational energies for the proteinogenic amino acids through explicitly correlated methods. Assessment of density functional methods, J. Chem. Theor. Comput. 12 (2016) 444–454.

[11] D. Řeha, H. Valdes, J. Vondrášek, P. Hobza, A. Abu-Rizig, B. Crew, M.S. de Vries, Structure and IR spectrum of phenylalanyl–glycyl–glycine tripetide in the gas-phase: IR/UV experiments, ab initio quantum chemical calculations, and molecular dynamic simulations, Chem. Eur J. 11 (2005) 6803–6817.

[12] H. Valdes, K. Pluháčková, M. Pitonák, J. Řezáč, P. Hobza, Benchmark database on isolated small peptides containing an aromatic side chain: comparison between wave function and density functional theory methods and empirical force field, Phys. Chem. Chem. Phys. 10 (2008) 2747–2757.

[13] L. Goerigk, A. Karton, J.M.L. Martin, L. Radom, Accurate quantum chemical energies for tetrapeptide conformations: why MP2 data with an insufficient basis set should be handled with caution, Phys. Chem. Chem. Phys. 15 (2013) 7028–7031.

[14] M. Rossi, S. Chutia, M. Scheffler, V. Blum, Validation challenge of density-functional theory for peptides−example of Ac-Phe-Ala$_5$-LysH$^+$, J. Phys. Chem. 118 (2014) 7349–7359.

[15] Y.K. Kang, H.S. Park, Exploring conformational preferences of alanine tetrapeptide by CCSD(T), MP2, and dispersion-corrected DFT methods, Chem. Phys. Lett. 702 (2018) 69–75.

[16] L. Goerigk, S. Grimme, Efficient and accurate double-hybrid-meta-GGA density functionals−evaluation with the extended GMTKN30 database for general main group thermochemistry, kinetics, and noncovalent interactions, J. Chem. Theory Comput. 7 (2011) 291–309.

[17] E. Brémond, I. Ciofini, J.C. Sancho-García, C. Adamo, Nonempirical double-hybrid functionals: an effective tool for chemists, Acc. Chem. Res. 49 (2016) 1503–1513.

[18] J.M.L. Martin, G. Santra, Empirical double-hybrid density functional theory: a 'third way' in between WFT and DFT, Isr. J. Chem. 60 (2020) in press.

[19] L. Goerigk, S. Grimme, A thorough benchmark of density functional methods for general main group thermochemistry, kinetics, and noncovalent interactions, Phys. Chem. Chem. Phys. 13 (2011) 6670–6688.

[20] M. Walker, A.J.A. Harvey, A. Sen, C.E.H. Dessent, Performance of M06, M06-2X, and M06-HF density functionals for conformationally flexible anionic clusters: M06 functionals perform better than B3LYP for a model system with dispersion and ionic hydrogen-bonding interactions, J. Phys. Chem. 117 (2013) 12590–12600.

[21] C. Ergene, K. Yasuhara, E.F. Palermo, Biomimetic antimicrobial polymers: recent advances in molecular design, Polym. Chem. 9 (2018) 2407–2427.

[22] R. Liu, X. Chen, Z. Hayouka, S. Chakraborty, S.P. Falk, B. Weisblum, K.S. Masters, S.H. Gellman, Nylon-3 polymers with selective antifungal activity, J. Am. Chem. Soc. 135 (2013) 5270–5273.

[23] R. Liu, X. Chen, S.P. Falk, B.P. Mowery, A.J. Karlsson, B. Weisblum, S.P. Palecek, K.S. Masters, S.H. Gellman, Structure−activity relationships among antifungal nylon-3 polymers: identification of materials active against drug-resistant strains of *Candida albicans*, J. Am. Chem. Soc. 136 (2014) 4333–4342.

[24] R. Liu, X. Chen, S.P. Falk, K.S. Masters, B. Weisblum, S.H. Gellman, Nylon-3 polymers active against drug-resistant *Candida albicans* biofilms, J. Am. Chem. Soc. 137 (2015) 2183–2186.

[25] L.A. Rank, N.M. Walsh, F.Y. Lim, S.H. Gellman, N.P. Keller, C.M. Hull, Peptide-like nylon-3 polymers with activity against phylogenetically diverse, intrinsically drug-resistant pathogenic fungi, mSphere 3 (2018) e00223-18.

[26] S.G. Hovakeemian, R. Liu, S.H. Gellman, H. Heerklotz, Correlating antimicrobial activity and model membrane leakage induced by nylon-3 polymers and detergents, Soft Matter 11 (2015) 6840–6851.

[27] R.D. Dennington II, T.A. Keith, J. Millam, GaussView, Version 6.0, Gaussian, Inc., Wallingford, CT, 2016.

[28] M.J. Frisch, et al., GAUSSIAN 09, Revision D.01, Gaussian, Inc., Wallingford, CT, 2013.

[29] Y. Zhao, D.G. Truhlar, The M06 suite of density functionals for main group thermochemistry, thermochemical kinetics, noncovalent interactions, excited states, and transition elements: two new functionals and systematic testing of four M06-class functionals and 12 other functionals, Theor. Chem. Acc. 120 (2008) 215–241.

[30] A.V. Marenich, C.J. Cramer, D.G. Truhlar, Universal solvation model based on solute electron density and on a continuum model of the solvent defined by the bulk dielectric constant and atomic surface tensions, J. Phys. Chem. B 113 (2009) 6378–6396.

[31] Y.K. Kang, B.J. Byun, Assessment of density functionals with long-range and/or empirical dispersion corrections for conformational energy calculations of peptides, J. Comput. Chem. 31 (2010) 2915–2923.

[32] BIOVIA Discovery Studio, Version 16, Dassault Systèmes Co., Waltham, Mass, 2015.

[33] Y.K. Kang, Ab initio MO and density functional studies on *trans* and *cis* conformers of *N*-methylacetamide, J. Mol. Struct. Theochem. 546 (2001) 183–193.

[34] W.J. Hehre, L. Radom, P.v.R. Schleyer, J.A. Pople, Ab Initio Molecular Orbital Theory, John Wiley & Sons, New York, 1986 (chapter 6).

[35] A. Halkier, T. Helgaker, P. Jørgensen, W. Klopper, H. Koch, J. Olsen, A.K. Wilson, Basis-set convergence in correlated calculations on Ne, N$_2$, and H$_2$O, Chem. Phys. Lett. 286 (1998) 243–252.

[36] J.P. Perdew, K. Schmidt, Jacob's ladder of density functional approximations for the exchange-correlation energy, AIP Conf. Proc. 577 (2001) 1.

[37] J.P. Perdew, A. Ruzsinszky, J. Tao, V.N. Staroverov, G.E. Scuseria, G.I. Csonka, Prescription for the design and selection of density functional approximations: more constraint satisfaction with fewer fits, J. Chem. Phys. 123 (2005), 062201.

[38] J.-D. Chai, M. Head-Gordon, Long-range corrected hybrid density functionals with damped atom–atom dispersion corrections, Phys. Chem. Chem. Phys. 10 (2008) 6615–6620.

[39] T. Schwabe, S. Grimme, Double-hybrid density functionals with long-range dispersion corrections: higher accuracy and extended applicability, Phys. Chem. Chem. Phys. 9 (2007) 3397–3406.

[40] S. Kozuch, J.M.L. Martin, DSD-PBEP86: in search of the best double-hybrid DFT with spin-component scaled MP2 and dispersion corrections, Phys. Chem. Chem. Phys. 13 (2011) 20104–20107.

[41] S. Grimme, S. Ehrlich, L. Goerigk, Effect of the damping function in dispersion corrected density functional theory, J. Comput. Chem. 32 (2011) 1456–1465.

[42] P. Enkhbayar, S. Damdinsuren, M. Osaki, N. Matsushima, HELFIT: helix fitting by a total least squares method, Comput. Biol. Chem. 32 (2008) 307–310.

[43] K. Möhle, R. Günther, M. Thormann, N. Sewald, H.-J. Hofmann, Basic conformers in β-peptides, Biopolymers 50 (1999) 167–184.

[44] E.N. Baker, R.E. Hubbard, Hyfrogen Bbonding in globular proteins, Prog. Biophys. Mol. Biol. 44 (1984) 97–179.

[45] R.P. Cheng, S.H. Gellman, W.F. DeGrado, β-Peptides: from structure to function, Chem. Rev. 101 (2001) 3219–3232.